EGTRIB Journal
JOURNAL OF
THE EGYPTIAN SOCIETY OF TRIBOLOGY
VOLUME 20, No. 3, July 2023, pp. 40 - 62 **ISSN 2090 - 5882**
(Received February 17. 2023, Accepted in final form April 30. 2023) **jest.journals.ekb.eg**

MECHANICAL AND TRIBOLOGICAL PROPERTIES OF POLYMETHYL METHACRYLATE MATRIX REINFORCED WITH NOVEL HYBRID ORGANIC AND INORGANIC NANO-FILLERS.

Hassan A. El-Sayed M.[1], Ali Eman M.[1], El-Sheikh M. N.[1], Rohim M. Nafea M.[1], Elkhouly Heba I.[2]

[1]Mechanical Dept., Faculty of Technology and Education, Beni-Suef University, Beni-Suef, EGYPT.
[2]Department of Mechanical Engineering, Faculty of Engineering, Beni-Suef University, Beni-Suef, EGYPT.

ABSTRACT

Polymethyl methacrylate (PMMA) possesses favorable properties such as a valuable physical characteristic, low cost, and its ease and aesthetic fabrication. However, it suffers from low hardness and tribological properties in denture base applications. In this work, the mechanical and tribological properties of PMMA reinforced with organic, inorganic, and hybrid of organic/inorganic nanoparticles (NPs) were investigated. The used organic fillers were date seed (DS) NPs and inorganic fillers were titanium dioxide (TiO_2) NPs. TiO_2 and DS NPs were characterized by transmission electron microscope (TEM). PMMA-based non-hybrid and hybrid nanocomposites were fabricated by using a self-curing method. To fabricate the non-hybrid composites of C1 and C2, TiO_2 and DS NPs were added at a constant weight fraction (wt. %) of 1.2 to PMMA, respectively. For manufacturing hybrid nanocomposites, C1 was reinforced by 0.1, 0.2, 0.3, 0.4, and 0.5 wt. % DS NPs. Also, C2 was reinforced with TiO_2 NPs at the same loading content of 0.1, 0.2, 0.3, 0.4, and 0.5 wt. %. Unfilled PMMA, C1, C2, C1/0.4 wt. % DS NPs, and C2/0.4 wt. % TiO_2 NPs were analyzed by Fourier transform infrared (FTIR) technique. Vickers hardness number (VHN), wear rate, and coefficient of friction (COF) tests were conducted to study the effect of hybrid NPs content on the mechanical and tribological properties of PMMA. The worn surfaces of rubbed specimens after the wear test were imaged by scanning electron microscope (SEM).

The experimental results proved that the mechanical and tribological characteristics of unfilled PMMA were significantly improved at content of 1.2 wt. % DS and TiO_2 NPs for C1 and C2, respectively. Hence, the hybrid nanocomposites that reinforced with 0.4 wt. % DS or TiO_2 NPs recorded a distinct mechanical and tribological behavior among other filler content. Also, the hybrid nanocomposites of C2/0.4 wt. % TiO_2 NPs showed significant improvement by 14.12, 16.66, and 2.96 % in the VHN, wear rate, and COF, respectively compared to the hybrid nanocomposites of C1/0.4 wt. % DS NPs. Finally, samples costing study proved that the unit cost of the hybrid

nanocomposites of C2/0.4 wt. % TiO_2 NPs is lower than that of the hybrid nanocomposites of C1/0.4 wt. % DS NPs by 47.61%.

KEYWORDS
PMMA; Hybrid nanocomposites; Organic nanofillers; Inorganic nanofillers; Mechanical properties; Tribological properties.

INTRODUCTION

PMMA is widely used as a denture base material since the 1930s because it has many significant advantages such as simple manufacturing and repair techniques, ease of handling and processing, low cost, and acceptable physical and mechanical properties, [1- 3]. Unfortunately, this material has some inherent shortcomings, which finally cause failure of prosthesis during clinical service, [4, 5]. Even after the modifications, PMMA resin is far from a good material as denture base material and requires more studies to provide an acceptable material, [6, 7]. Generally, PMMA denture base material fractures when loaded under flexural or impact forces that exceeding its mechanical capacity, [8- 10]. To improve the mechanical characteristics of PMMA, several attempts have been conducted by adding various types of fibers and nanofillers, [11].

Nowadays, nanotechnology has been applied in dental applications in which various researches have been employed to overcome the mechanical performance drawbacks of denture base materials, [12]. Several researches have been focused on enhancing of PMMA properties in all curing methods by incorporation of nanofillers in its composition, [13, 14]. Homogenous distribution of reinforcement material, as a filler in the nanometer scale, in PMMA, as matrix material, and interfacial interaction between them, led to improve the nanocomposites properties, [15, 16]. Polymeric nanocomposites characteristics depend on the type of incorporated NPs and their size, shape, concentration, and interaction with the polymer matrix, [17]. NPs that have a small size and high specific surface area show ideal performance and excellent features compared to conventional materials. Numerous studies shows that a wide spread of nanomaterials such as silver NPs, zinc oxide (ZnO) nanostructures, zirconium dioxide (ZrO_2) nanotubes, silica NPs, and carbon nanotubes are incorporated with PMMA to obtain denture base materials with enhanced mechanical properties, [18- 21].

Among these additives, ZrO_2 NPs are known for their inherent suitable properties. Previous studies emphasized an enhancement of the physical and mechanical properties of PMMA/ZrO_2 nanocomposite for denture base materials application, [14, 22]. It was found that adding of 3- 5 wt. % ZrO_2 NPs to PMMA nanocomposites showed improved fracture toughness, flexural strength, and surface hardness, [23]. Also, tensile, fatigue strength, and wear resistance of acrylic PMMA resin were improved after incorporating the modifying ZrO_2 NPs, [24]. Moreover, mechanical and tribological performance of self-cured PMMA reinforced by alumina (Al_2O_3) nanowires and ZrO_2 NPs for denture applications were studied by Hassan *et al*. They found that the mechanical and tribological properties were enhanced by adding Al_2O_3

nanowires and ZrO_2 NPs up to 0.5 and 0.7 wt. %, respectively, [14]. Also, Jasim *et al.* found that adding of Al_2O_3 NPs to PMMA improved the flexural strength and decreased the thermal expansion coefficient of acrylic resin, [25].

TiO_2 NPs are among the biocompatible nontoxic materials, [11]. These NPs have resistance against corrosion, chemical stability, and high refractive index, [26, 27]. As reported by Sodagar *et al.*, flexural strength of PMMA/ TiO_2 composites was improved after adding of 0.5 and 1 wt. % TiO_2 NPs, [28]. Also, another study proved that TiO_2 NPs reduced the flexural strength without changing the flexural modulus, [29]. However, an enhancement of both elastic modulus and flexural strength were observed after addition of 0.5% TiO_2 NPs, as observed by Rashahmadi *et al.*, [30]. Recently, organic fillers are the most widely used in composites manufacturing because of their low preparation costs, as well as relatively high strength values to weight ratios can be obtained, [18]. Moreover, organic fillers are becoming increasingly popular as environmental friendly and renewable alternatives, [31]. Also, they can be obtained from recycled waste materials such as ajwa dates, pomegranate peels, [32], and fly ash, [33]. These materials have been incorporated into a variety of biomaterials in order to induce antimicrobial activity and improve the mechanical behavior, [34]. One of the most widely organic materials, DS NPs, which distinguished by their low density, low preparation costs, and high mechanical properties. Because of their effective properties, such as high chemical inertness and excellent mechanical performance, DS NPs are considered to be attractive reinforcement for polymer matrix composites, [35- 37]. A comparison of the effects of DS NPs as reinforcement material for medium-density polyethylene (MDPE) and polyethylene terephthalate (PET) was studied, [38]. This study concluded that the wear surface hardness characteristics of MDPE and PET were improved at 0.75 wt. % DS NPs.

Based on the previous literature surveys, ZrO_2, ZnO, TiO_2, and Al_2O_3 NPs had significant improving effect on the mechanical properties of PMMA, however there was a little data available related to their effect on the wear resistance and COF of PMMA acrylic resin, so further investigations were needed. Moreover, there are no studies that have yet been conducted to incorporate DS NPs into PMMA acrylic resin for denture base applications. Hence, this work was performed to evaluate the mechanical and tribological properties as well as economical effectiveness of PMMA reinforced with hybrid DS and TiO_2 NPs at various loading content of hybrid NPs.

EXPERIMENTAL WORK

Materials

In the present study, matrix material composed of powdered PMMA and MMA monomer as a liquid hardener that were supplied from Acrostone Dental & Medical Supplies Company, Cairo, Egypt. NPs of organic and inorganic materials such as DS and TiO_2 were introduced as reinforcement materials to enhance the mechanical and tribological properties of the composite. TiO_2 NPs were supplied from Nano Tech. Company, El-Giza, Egypt. Whereas DS NPs were prepared in Material Lab, Faculty of Technology and Education, Beni-Suef University, Egypt, as reported by Elkhouly

***et al*. [37]. DS was dried before being ground for 24 hours at 70 °C. Then, DS was milled in a ball milling machine for 140 hours to reach the nano-scale size. To check the nano size and morphology of TiO_2 and DS, TEM was employed by National Center for Research, Egypt.**

Nanocomposites Fabrication

Fig. 1 shows a flowchart of non-hybrid and hybrid nanocomposites preparation. In this work, self-curing technique was used to prepare the present C1 and C2, non-hybrid composites, and hybrid nanocomposites of C1/x DS NPs and C2/x TiO_2 NPs. Samples code of C1, C2, and x was introduced in Table 1. Non-hybrid composites of C1 and C2 were fabricated at a constant content of 1.2 wt. % of TiO_2 and DS NPs, respectively according to Ref., [39]. To prepare the hybrid nanocomposites, variable contents of x, which varies from 0.1 to 0.5 wt. % of DS and TiO_2 NPs, were added to C1 and C2, respectively. Generally, for manufacturing of hybrid and non-hybrid nanocomposites, TiO_2 or DS NPs were added to PMMA powder in a glass beaker. Then, the mixture was stirred continuously for 30 minutes in clockwise and counterclockwise to obtain a homogenous mixture, [14]. For completing the polymerization process according to self-curing technique, MMA monomer, as a liquid, was added to the mixture at 1:2.5 ratio, [40]. Non-hybrid and hybrid nanocomposites were then molded in a cylindrical tube which were kept in a vacuum system under pressure of 30 psi for 24 hours to obtain the samples without porosity. Finally, the specimens of 8 mm diameter and 25 mm length were prepared for further tests.

Table 1 Samples codes

Code	Code interpretation
C1	Non-Hybrid composite of PMMA/1.2 wt. % TiO_2 NPs
C2	Non-Hybrid composite of PMMA/1.2 wt. % DS NPs
x	Hybrid-nanofiller content (0.1, 0.2, 0.3, 0.4, and 0.5 wt. %)

Nanocomposites Characterization

In the present study, non-hybrid and hybrid nanocomposites of C1, C2, C1/x DS NPs, and C2/x TiO_2 NPs were characterized mechanically and tribologically. Mechanical characterization includes VHN test, while tribological characterization includes wear and COF Tests.

Vickers Microhardness Test

Vickers microhardness test was conducted to estimate the VHN of the present nanocomposites. According to ASTM E384-99, Vickers microhardness test was don under testing load of 100 g for a dwell time of 10 s. VHN was calculated as follows:

$$VHN = 1854.4\ (\frac{P}{d^2}) \quad (1)$$

where: P is the applied load, gf, and d is the mean diagonal length of the indentation, µm. To get accurate test results, each specimen surface was tested by five indentations from center to the external periphery of the sample and average values were reported.

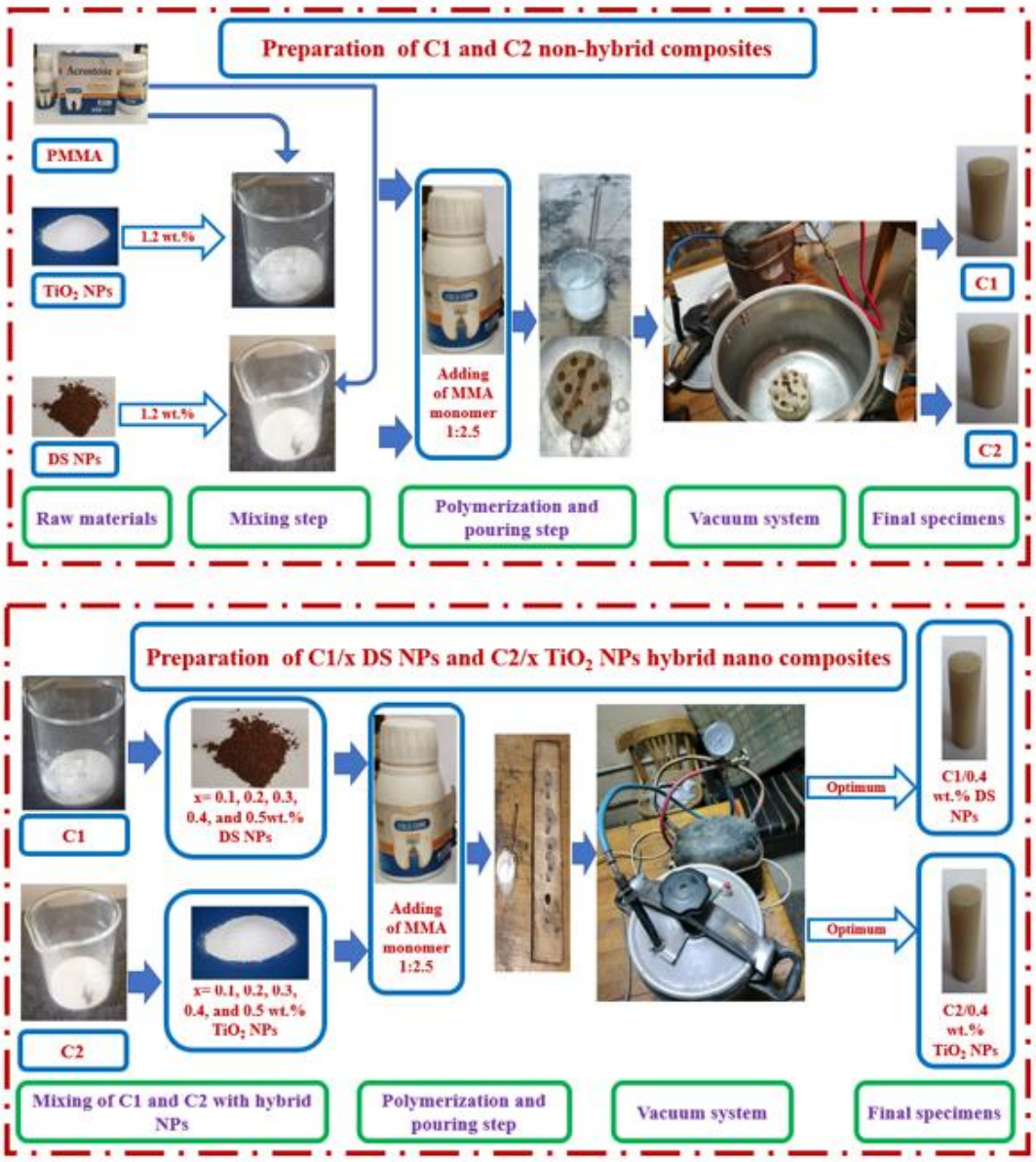

Fig. 1 Flowchart of non-hybrid and hybrid nanocomposites preparation.

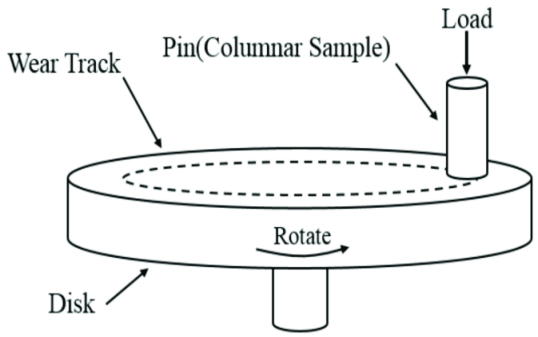

Fig. 2 Pin-on-disc schematic diagram, [41].

Wear Test

Wear test was carried out under dry sliding conditions using a pin-on -disk test rig, as indicated in Fig. 2, according to ASTM G 99 standard [42, 43]. The sliding counterface in the pin-on-disk setup was a carbon steel disc that has a surface roughness (Ra) of 1.41µm, and surface hardness of 58-62 HV. Specimens were loaded by 30 N at a constant sliding speed and sliding distance of 1.2 m/s and 450 m, respectively. Before and after the wear test, the specimen was weighed by electronic balance, which has accuracy of ±0.1 mg. Wear rate is the difference between the initial and final weights divided by sliding distance. Each specimen was tested three times and averaged values wear reported to obtain sturdy results.

COF Test

At the same parameter of wear test, COF of the non-hybrid and hybrid nanocomposites of C1, C2, C1/x DS NPs, and C1/x TiO_2 NPs was measured during the wear test, as indicated in Fig. 2. COF was calculated as follows:

$$\text{COF } (\mu) = \frac{F}{N} \quad (2)$$

Where F is the frictional force and N is the normal load. Friction force was measured by a load cell of 40 kg and recorded each one millisecond by a calibrated data logger that connected with a computer. The averaged value of three tests of each specimen was reported.

Microstructure and Worn Surfaces Examination.

The microstructure and worn surfaces of the present hybrid and non-hybrid composites were examined and imaged by SEM. Furthermore, the distribution of the NPs within the hybrid nanocomposites was imaged. Also, after the wear and friction tests, worn surfaces of hybrid and non-hybrid composites were examined imaged to study the occurred wear mechanism and effect of hybrid NPs content on the mechanical tribological properties of the PMMA.

FTIR Characterization

FTIR spectrophotometer was recorded using a Bruker (Vertex 70 FTIR-Raman) spectrophotometer. It was done for scanning the pure PMMA, non-hybrid composites of C1 and C2, and hybrid nanocomposites of C1/0.4 DS NPs and C2/0.4 TiO_2 NPs. Infrared light was employed to scan the molecular structure of the test samples. Also, the utility of infrared spectroscopy arises due to different chemical structures that produce different spectral.

RESULTS AND DISCUSSION

Examination and Characterization of NPs

As shown in Fig. 3 a TEM image, the TiO_2 NPs have an oval shape, a clumped distribution, and an average size of ~23 nm. On the other hand, TEM analysis of prepared DS NPs proved that the particles were successfully converted into nano-sized scale via ball-milling processing and have an average size of ~ 4 nm, as shown in Fig. 3 b. Although the form and scale of TiO_2 and DS NPs are highly variable in these images, each particle appears essentially spherical. Similar observations about the shapes of NPs have been previously reported, [44]. These shape and size variations lead to enhanced mechanical properties for the reinforced materials.

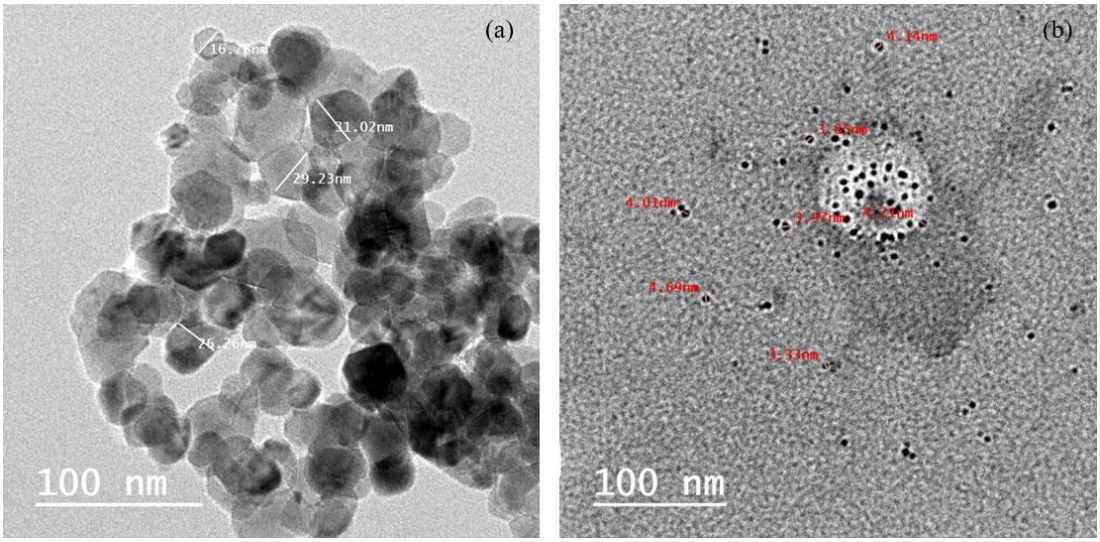

Fig. 3 TEM imaging of: a) as recived TiO_2 NPs, b) prepared DS NPs.

FTIR Analysis

Figure 4 shows the recorded FTIR spectra of the characteristic vibration bands of pure PMMA, C1, C2, C1/0.4 wt. % DS NPs, and C2/0.4 wt. % TiO_2 NPs. Firstly, the bands of pure PMMA are as following. The band at 1,444 cm^{-1} could be attributed to the bending vibration of the C–H bonds from – CH_3 group. The absorption band 2,819 cm^{-1} could be assigned to C-H bond stretching vibration – CH_2 groups, while that appeared at 1,730 cm^{-1} (C=O) and 1,380 cm^{-1} (C–O). Moreover, there is a vibration band at 1,150 cm^{-1} represents C–O and stretching bands at 975 cm^{-1} and 831 cm^{-1} C–C which belong to the ester group for PMMA spectrum, [45]. Also, there are absorption bands at 2947 cm^{-1} and 2960 cm^{-1}, which could be attributed to characteristic stretching and bending vibrations of the –OH group. A distinct absorption band 1,199 cm^{-1} could be attributed to C–O–C stretching vibration. Also, it could be considered that the band at 752 cm^{-1} showed O-C=O, while the absorption band at 1,741 cm^{-1} revealed the presence of the acrylate carboxyl group.

The doping of the TiO_2 / DS NPs could be assigned by studying the formation of new peaks, or various shoulders, sharpening or change in the shape, shift of the absorption bands, or intensity of the existing vibration bands in FTIR spectra as seen in Fig. 4. For instance, Ti-O-C vibration band occurs at 831 cm^{-1} and 975 cm^{-1} revealed to the formation of nanocomposites. These bands seem to be characteristic of the presence of TiO_2 nanoparticles, as previously declared, [47] . After the addition of TiO_2 / DS NPs the band at 1444 cm^{-1} split into two peaks, the older one 1444 cm^{-1} and a new shoulder at 1450 cm^{-1}. Also, the band of 1380 cm^{-1} was increased at the PMMA/TiO_2 NPs and PMMA/DS NPs as shown in FTIR spectra, which could be assigned as an indication for PMMA and TiO_2 / DS NPs interaction. Moreover, an increase was observed in the intensity of the stretching band at 1583 cm^{-1} which related to the carboxyl group (– COO^-) of the nanocomposites. Notably, the intensity of 2844 cm^{-1} band of (– CH) increased at the nanocomposites, which reflects the PMMA/TiO_2 NPs and PMMA/DS NPs interactions. Meanwhile, O-H increased with NPs addition, while results showed that O-H intensity decreased with TiO_2 addition, [48].

Overall, DS NPs have smaller size than TiO_2 NPs which led to more intensity of PMMA/DS NPs FTIR bands than those of PMMA/TiO_2 NPs. This result agrees with Rahman *et al*. who found that bands height increased with decreasing the NPs size, [49].

As can be seen, with the embedding of hybrid NPs into PMMA, interaction of the oxygen atom in the carbonyl group (C=O) and the hydroxyl groups (OH) is the possible interaction between the hybrid NPs and PMMA. By the addition of hybrid NPs at C1/0.4 wt. % DS NPs, and C2/0.4 wt. % TiO_2 NPs, two differences appeared in FTIR spectra. The first, a shift from 2960 cm^{-1} to 2952, and 2950 cm^{-1}, respectively. Also, from 1741 cm^{-1} to 1737, and 1735 cm^{-1}, respectively, indicate well TiO_2 and DS interaction with PMMA. That agrees with Aframehr, *et al.* who found that bands shifted toward lower frequencies which indicates NiO interaction with PI matrix, [50]. Generally, if the shift happened toward lower wavenumber, it means the interaction between the two phases is strong and leads to an increase in the strength of the bonds between them, [50]. The second change was a decrease of the intensity of the bands of the –OH group at 2952, and 2950 cm^{-1}), and of the acrylate carboxyl group in 1737, and 1735 cm^{-1} which indicate well interaction between the hybrid NPs and PMMA. This result agrees with Aframehr, *et al.* who proved that a decrease in intensity of the free carbonyl indicates a good interaction between NiO and PI matrix, [50].

It is obvious that the interaction between hybrid NPs and PMMA at C2/0.4 wt. % TiO_2 NPs is more than at C1/0.4 wt. % DS NPs as the bands shifted toward lower wavelengths and their intensity was the lowest.

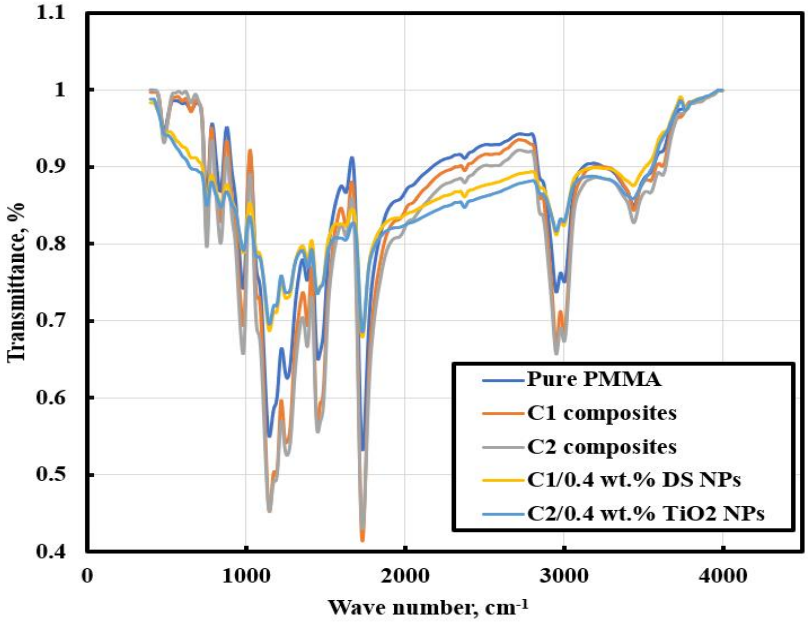

Fig. 4 FTIR spectroscopy.

Microstructure Observations of Produced non-hybrid and Hybrid Nanocomposites.

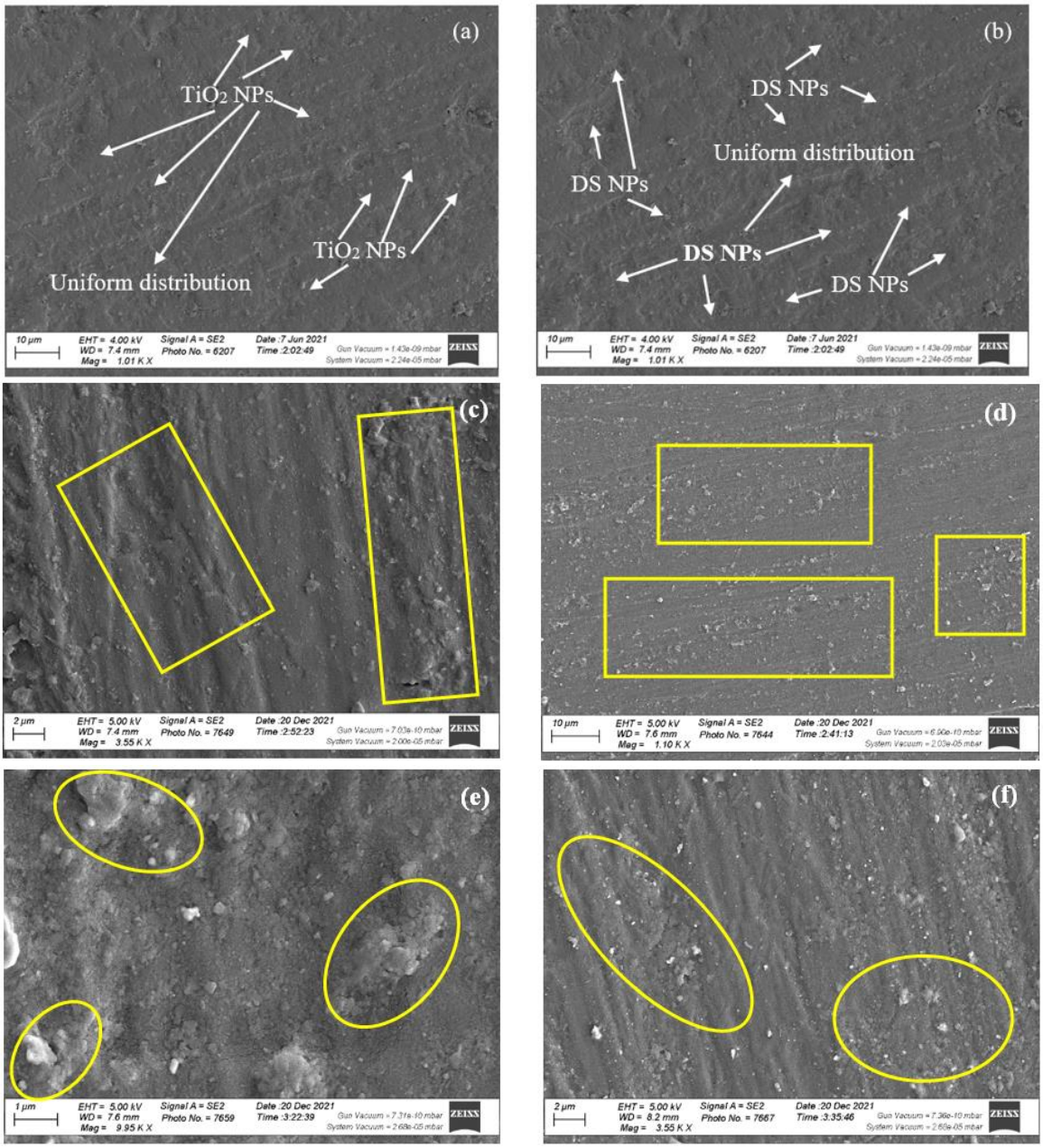

Fig. 5 SEM of: a) non-hybrid composites of C1, b) non-hybrid composites of C2, c) hybrid-nanocomposites of C1/0.4 wt. % DS NPs, d) hybrid-nanocomposites of C2/0.4 wt. % TiO_2 NPs, e) hybrid-nanocomposites of C1/0.5 wt. % DS NPs, and f) hybrid-nanocomposites of C2/0.5 wt. % TiO_2 NPs.

The microstructure of non-hybrid composites of C1 and C2 were explored by SEM, as shown in Fig. 5 a, b, respectively. In these images, an excellent distribution of TiO_2 and DS NPs at 1.2 wt. % within PMMA was observed. The uniform distribution of NPs within the PMMA leads to increasing the mechanical and tribological properties of the PMMA composites. Moreover, the microstructure of hybrid nanocomposites of C1/0.4 wt. % DS NPs and C2/0.4 wt. % TiO_2 NPs were shown in Fig. 5, c and d,

respectively. As shown in Fig. 5, c and d, the hybrid NPs at 0.4 wt. % of DS and TiO_2 were observed to be highly uniformly distributed within the C1 and C2 non-hybrid composites, as indicated in the regions marked by the yellow rectangles. After increasing the hybrid NPs content up to 0.5 wt. %, some agglomerations of NPs appeared in the microstructure images of the hybrid nanocomposites, as shown by the areas marked by the yellow ovals in Fig. 5, e and f. The well dispersion of 0.4 wt. % NPs within the non-hybrid composites of C1 and C2 was the reason for the uniform distribution of the loads. The well distribution of the content of 0.4 wt. % NPs was a major reason for the uniform distribution of the loads into the PMMA matrix material. In addition to that, these loads can also be transferred regularly to the reinforcement NPs, thus improving the mechanical and tribological properties of the nanocomposites. Therefore, the hybrid nanocomposites of C1/0.4 DS NPs and C2/0.4 TiO_2 NPs showed the highest mechanical and tribological properties, as going to be clear later.

Mechanical Properties

This section illustrates the effect of hybrid NPs addition on the VHN of the present non-hybrid and hybrid nanocomposites. Figure 6 represents the microhardness results of the present non-hybrid and hybrid nanocomposites, respectively. Materials for denture base applications should have an abrasion resistance to abrasive denture cleansers, foods, and general applied forces, [51]. Also, higher hardness of denture base materials will reduce the abrasive wear mechanism. For the non-hybrid composites of C1 and C2, DS and TiO_2 NPs at 1.2 wt. % enhanced the VHN of the pure PMMA by 39.56 and 67.47 %, respectively, as shown in Fig. 6 a.

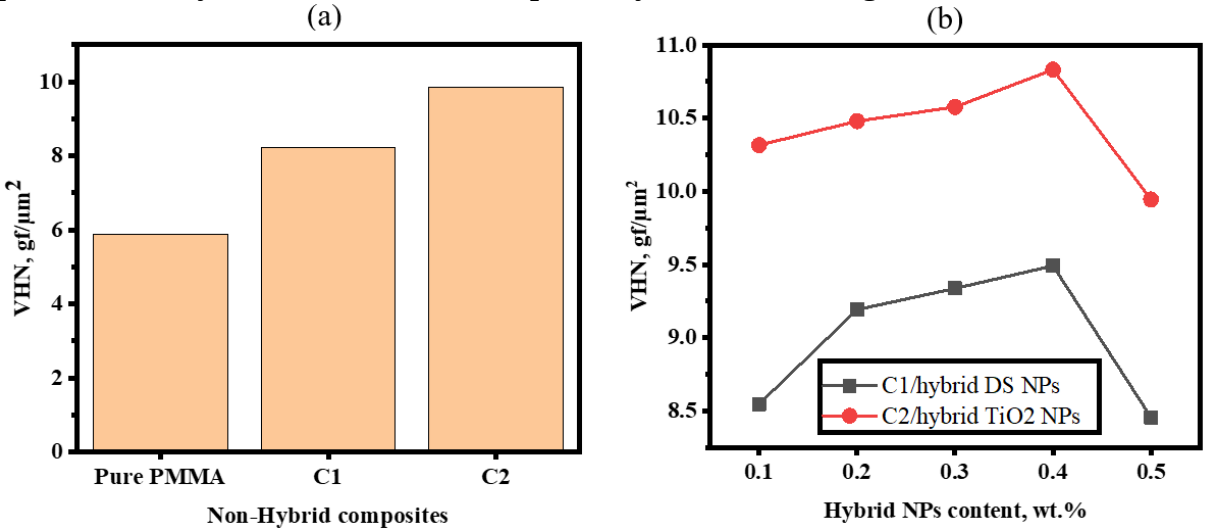

Fig. 6 Microhardness results: a) pure PMMA, C1, and C2 non-hybrid composites, b) C1/0.4 wt. % DS NPs and C2/0.4 wt. % TiO_2 NPs hybrid nanocomposites.

The significant enhancement of the microhardness number of the present PMMA and its nanocomposites was attributed to the strong interfacial adhesion bond between the nano reinforcement materials and PMMA. Moreover, DS and TiO_2 NPs act as strengthening materials of the PMMA that led to improvement of the load carrying capacity. Also, the molecular-level dispersion of DS and TiO_2 NPs up to content of 1.2

wt. % in PMMA may be the reason of higher microhardness of these nanocomposites. The present microhardness results of PMMA/TiO_2 NPs composites are consistent with the microhardness results of the same composite that obtained by Alamgir *et al.*, [52]. Whereas DS NPs, as reinforcement, achieved the highest microhardness number of PMMA compared to TiO_2 NPs.

Microhardness results of hybrid nanocomposites of C1/x DS NPs and C2/x TiO_2 NPs were plotted in Fig. 6 b. According to the VHN variations, as indicated in Fig. 6 b, DS NPs increased the VHN of non-hybrid composite C1 by 4.01, 11.85, 13.61, 15.49, and 2.89 % at 0.1, 0.2, 0.3, 0.4, and 0.5 wt. % content, respectively. Also, TiO_2 NPs increased the VHN of non-hybrid composite C2 by 4.60, 6.27, 7.25, 9.84, and 0.84 % at 0.1, 0.2, 0.3, 0.4, and 0.5 wt. % content, respectively. The optimum VHN of hybrid C1/x DS NPs and C2/x TiO_2 NPs nanocomposites was at 0.4 wt. % NPs content. This may be because of the too small size of the DS NPs, ~4 nm, which led to their good incorporation with TiO_2 NPs and PMMA. Addition of hybrid NPs content beyond 0.4 wt. % up to 0.5 wt. % showed significant decrease in VHN which could be clearly understood from Fig. 6 b. This may be due to the agglomerated NPs that led to porosity formation at high content of NPs addition. Despite the decrease in the VHN values after increasing the hybrid NPs content from 0.4 wt. %, the VHN of the hybrid nanocomposites at 0.5 wt. % of NPs content is still higher than that of VHN of C1 and C2 non-hybrid composites.

Figure 7 shows the details of the VHN that distributed on the optimum samples surface by mapping hardness analysis. Generally, microhardness maps emphasize the VHN distribution on X and Y axes. Therefore, as shown in Fig. 7 a, VHN of the pure PMMA was 5.88 gf/μm^2, which is determined by the yellow color on the map, was distributed regularly on the sample surface. Also, after adding TiO_2 and DS NPs at 1.2 wt. %, VHN of pure PMMA increased up to 8.21 and 9.86 gf/μm^2 for the non-hybrid composites of C1 and C2, respectively. This is for the areas marked by green and yellow colors that distributed on the hardness maps, as shown in Fig. 7 b and c, respectively.

Indeed, experimental results of VHN for the hybridized samples at 0.4 wt. % NPs content showed a significant improvement compared to the pure PMMA and the non-hybridized samples of C1 and C2. The VHN distributed by values of 9.49 and 10.83 gf/μm^2, marked by yellow color, on the hybrid nanocomposite maps at 0.4 wt. % of DS and TiO_2 NPs content, as shown in Fig. 7 d and e, respectively. The improvement in VHN results of the non-hybrid and hybrid nanocomposites may be due to the improvement of the properties and strengthening of PMMA that occurred at the molecular level by reinforcing with NPs, [53, 54]. Moreover, the uniform distribution of the NPs within the PMMA matrix material as well as possess high specific surface area led to an increase in the effectiveness of stress transmission to the NPs easily. This result is in good agreement with those reported in Refs., [14, 55].

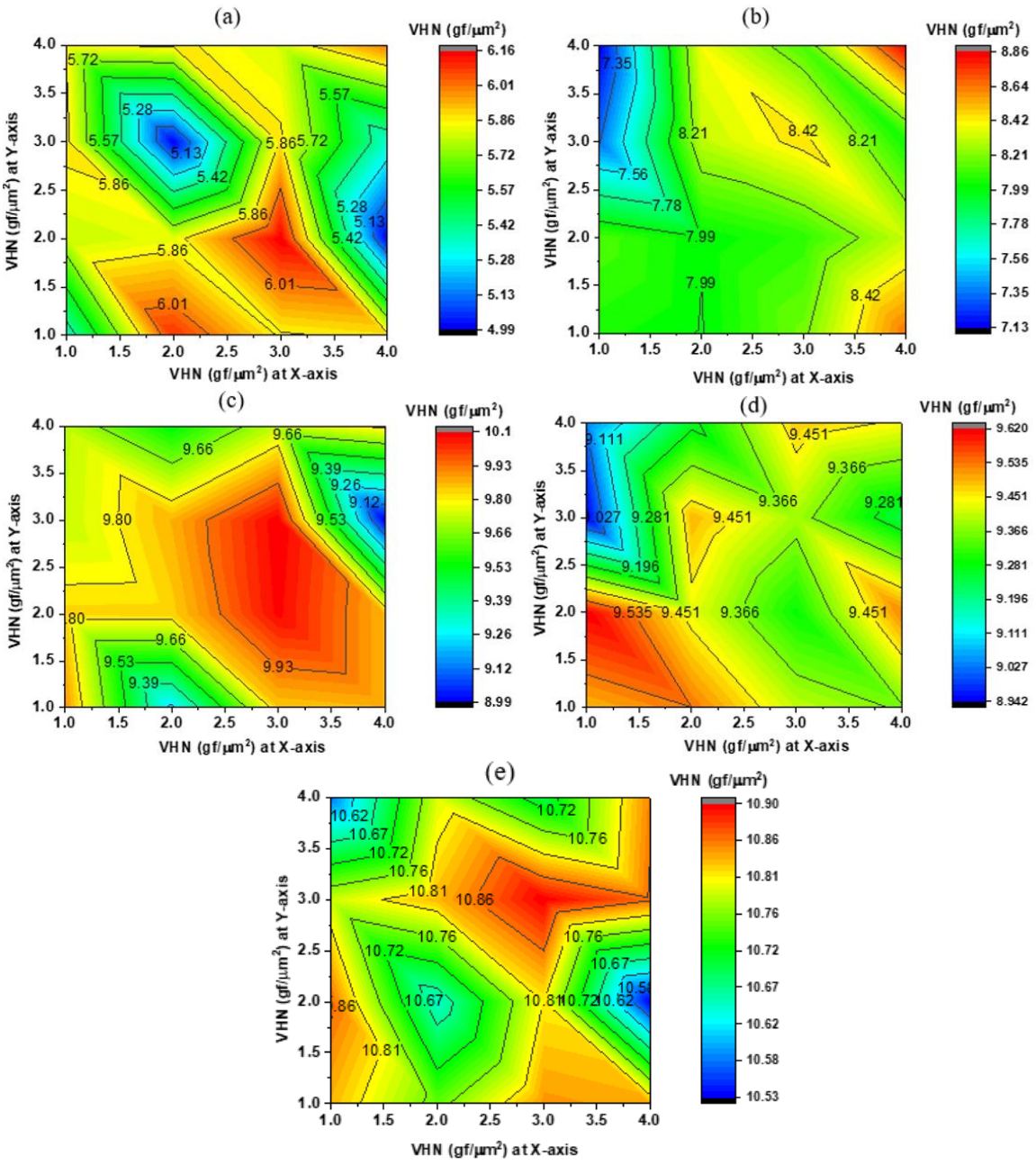

Fig. 7 Mapping of microhardness results: a) Pure PMMA, b) C1 non-hybrid nanocomposites, c) C2 non-hybrid nanocomposites, d) C1/0.4 wt. % DS NPs hybrid nanocomposites, and e) C2/0.4 wt. % TiO_2 hybrid nanocomposites.

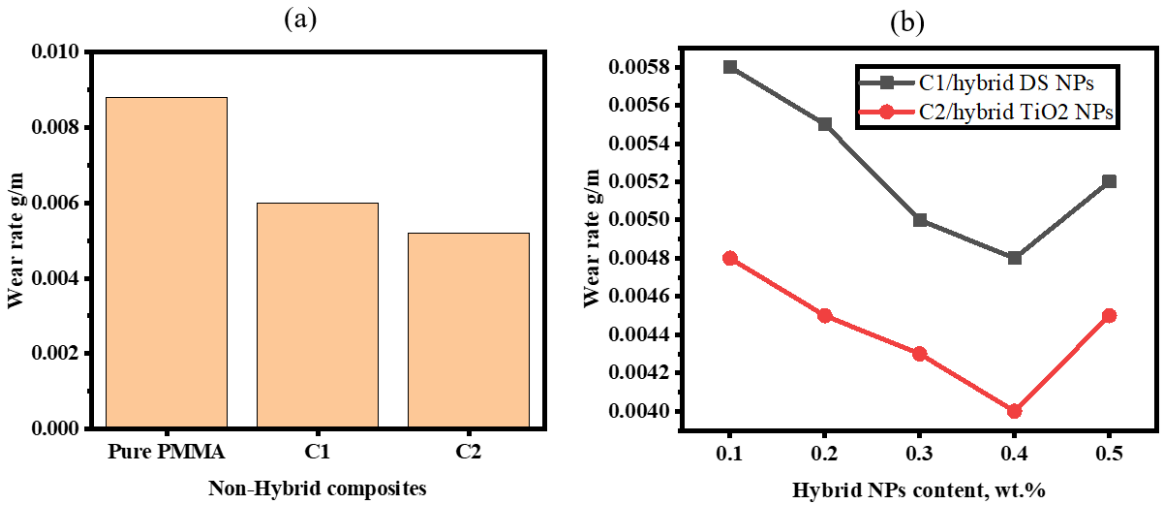

Fig. 8 Wear rate of the tested nanocomposites. a) pure PMMA, C1, and C2 non-hybrid composites, b) C1/0.4 wt. % DS NPs and C2/0.4 wt. % TiO_2 NPs hybrid nanocomposites.

Tribological Properties

Due to the close similarity of the PMMA's physical and mechanical properties with the properties of human dentin, the PMMA is widely used in denture base applications, [56]. PMMA is rarely used in tribological applications because it has a relatively low wear resistance compared to other tribological materials, [57]. Therefore, it is very important to seize the opportunity to study the tribological properties of the PMMA. Here, the effect of organic and inorganic NPs, as hybrid nanofillers, on the tribological performance of PMMA was studied at low loading contents. Thus, the fabricated specimens were rubbed against carbon-steel counterpart under applied load of 30 N at constant sliding speed and sliding distance of 1.2 m/s and 450 m, respectively.

Figure 8 shows the wear rate as a function of hybrid organic and inorganic NPs content. It was declared that the pure PMMA recorded the highest wear rate value compared to non-hybrid and hybrid nanocomposites. After addition of TiO_2 and DS NPs up to 1.2 wt. %, wear rate significantly improved by 31.81 and 40.9 % for the non-hybrid composites of C1 and C2, respectively (Fig. 8 a). This may be due to good distribution of TiO_2 and DS in PMMA matrix material that led to reducing the wear rate by protection of PMMA matrix from abrasion and fracture during the wear mechanism, as indicated by SEM images in Figs 10 b and c, respectively. These results were in accordance with Rohim *et al* study, [58]. They reported a 58.33% reduction in wear rate for the PMMA reinforced with NPs composites compared to the unfilled PMMA matrix material.

The wear rate curves of hybrid C1/x DS NPs and C2/x TiO_2 NPs nanocomposites were displayed in Fig. 8 b. It can be noticed that the behavior of the wear curves decreases significantly with the increase of the hybrid NPs content up to 0.4 wt. %. As for the hybrid nanocomposites of C1/x DS NPs, wear rate of non-hybrid composite C1 reduced by 3.33, 8.33, 16.66, and 20 % at 0.1, 0.2, 0.3, and 0.4 wt. % DS NPs,

respectively. Similarly, the wear rate of the non-hybrid composite, C2, decreased significantly by 7.69, 13.46, 17.30, and 23.07 % at 0.1, 0.2, 0.3, and 0.4 wt. % TiO_2 NPs, respectively. The improvement in the wear rate of the hybrid nanocomposites compared to the non-hybrid composites may be due to the increase in the surface mechanical properties of these hybrid nanocomposites.

Also, the hybrid NPs size that are used as reinforcement materials play an important role in improving the wear rate of these nanocomposites. For this reason, the interfacial adhesion bonding between the hybrid NPs and the matrix PMMA is improved at the molecular level due to the small size of hybrid NPs. It is noticed that there is a strong relationship between the wear rate and hardness number according to Archard equation, [59]. Upon the microhardness results of the present non-hybrid and hybrid nanocomposites, wear resistance of PMMA recorded the highest value at 1.2 wt. % NPs content, for non-hybrid composites, and 0.4 wt. % for hybrid nanocomposites. After increasing the hybrid NPs content up to 0.5 wt. %, the behavior of the wear rate curves began to increase compared to the optimum NPs content at 0.4 wt. %, but it was better than the non-hybrid composite of C1 and C2. This may be attributed to the agglomeration of NPs, which occurred at higher concentrations.

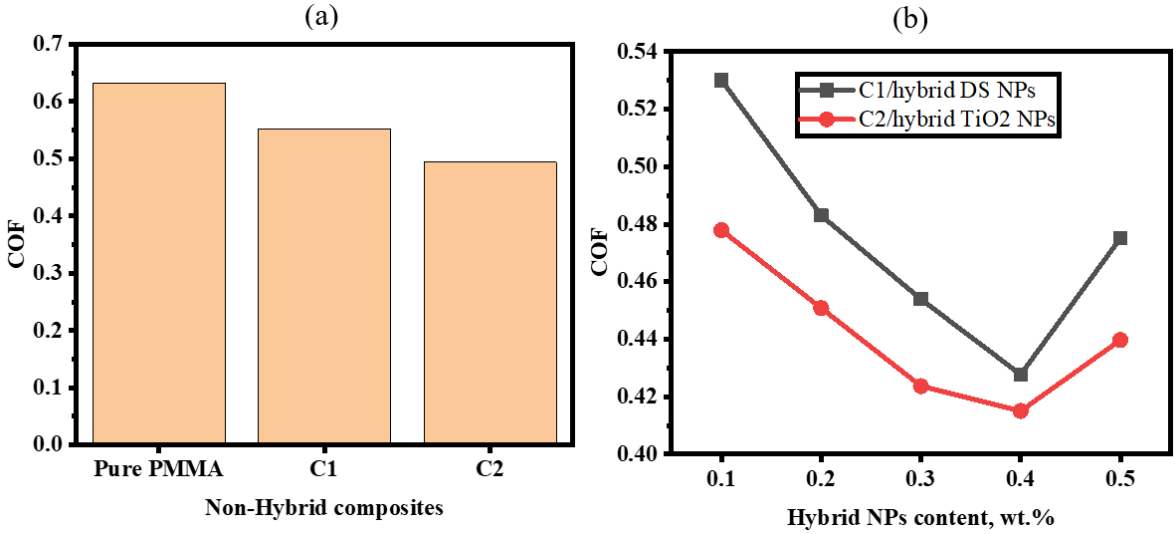

Fig. 9 COF of the tested nanocomposites. a) pure PMMA, C1, and C2 non-hybrid composites, b) C1/0.4 wt. % DS NPs and C2/0.4 wt. % TiO_2 NPs hybrid nanocomposites.

Amongst important tribological properties that must be considered in denture base applications are the friction coefficient properties. COF was measured during the wear test. According to the variations of COF, experimental results of the friction test showed a significant improvement at 1.2 wt. % of TiO_2 and DS NPs content compared to pure PMMA, as shown in Fig. 9 a. It was declared that the unfilled PMMA achieves the largest value of the COF. Therfore, COF of PMMA was enhanced by 12.81, and 21.87 % for non-hybrid composites of C1 and C2, respictively. This improvement in the COF results may be attributed to the small size of the NPs as well as their good

distribution, which act as self-lubricating materials on the PMMA matrix material surface. It is worth noting that the improvement percentage in the COF of unfilled PMMA after adding of 1.2 wt. % DS NPs was close to double the improvement percentage after adding 1.2 wt. % TiO_2 NPs. This is may be due to the samaller size of DS NPs than that of TiO_2 NPs.

As for the hybrid nanocomposites, it was observed that the friction coefficient of C1 and C2 decreased clearly with the increase of the hybrid NPs content up to 0.4 wt. %. Therefore, the optimum result of the frictional behavior was achieved at 0.4 wt. % NPs content. Nevertheless, it may be noticed that the hybrid nanofiller content when increased up to 0.5 wt. %, led to a regression of the COF behavior imrovement, as shown in Fig. 9 b. By examining the obtained experimental results, the COF of C1 was enhanced by 3.93, 12.45, 17.72, and 22.47 % at 0.1, 0.2, 0.3, and 0.4 wt. % DS NPs, respectively.

Also, the similar trends of curves were obtained by testing the hybrid nanocomposites of C2/x TiO_2 NPs. Hence, COF of C2 was significantly reduced by 3.33, 8.81, 14.3, and 16.05 %, at 0.1, 0.2, 0.3, and 0.4 wt. % TiO_2 NPs, respectively. Generally, the hybrid TiO_2 NPs /DS NPs has a prominent role to reduce the COF of C1 and C2 composites. This may be attributed to the hybrid TiO_2/DS NPs acts as a self-lubricating film on the contact area that reduced friction between the rubbing surfaces. Furtheremore, the hybrid NPs dispersion within the PMMA matrix material increases the grain refinement that leads to improvement the elasticity of the hybrid nanocomposite according to the Hall-Petch relation that reduces plasticity, [60]. As a result, an improvement in the hybrid nanocomposite stiffness and the reduction in indentation depth during rubbing surfaces were done, which reduces the deformation and wear debris, [61].

Worn Surfaces Examination.

To study and examine the wear and friction mechanisms, worn surface of the selected specimens was scanned and imaged after rubbing againist carbon-steel disc by SEM. It known that the worn surfaces of the scanned specimens clearly reflect the TiO_2 and DS NPs loading-dependent wear behavior. The worn surface details of unfilled PMMA, C1, C2, C1/0.4 wt. % DS NPs, and C2/0.4 TiO_2 NPs, respectively were introduced in Fig. 10. As indicated in Fig. 10 a, the detailed image of the wear marks of unfilled PMMA proved that the wear tracks formed on the specimens surfaces. Also, it can be obviously noticed that the contact surface area of unfilled PMMA specimen exhibits rougher texture that leds to spread of the wear and ploughed marks on the worn surface. Therefore, the wear mechanism was distinct with adhesive and ploughing wear. Due to the increased softening of the unfilled PMMA surface, which caused by the high temperature between the PMMA surface and asperities of carbon-steel disc, significant adhesive wear occurred. Also, the fractuers and ploughed zones were caused due to the penetration of abrasive asperities counterface easily into the unfilled PMMA, which led to occurrence of microploughing and microcutting on the worn surface. Furthermore, the weak layers that removed from the unfilled PMMA surface led to an increase in the shear resistance and, consequently, the COF and

wear rate. Moreover, the surface toughness of the unfilled PMMA decreased due to the increased surface roughness resulting from brittle failure during the rubbing process, which usually raises the wear rate and COF.

On the other hand, after addition of 1.2 wt. % TiO_2 and DS NPs, the worn surfaces of C1 and C2 non-hybrid composites had less ploughed marks than that of the unfilled PMMA, as illustirated in Figs 10 b and c, respictively. Due to the good distribution of TiO_2 and DS NPs at 1.2 wt. % for C1 and C2 non-hybrid composites, as well as the mechanical properties improvement, the worn surfaces showed less wear and ploughed marks compared to the pure PMMA. As a result, the wear rate and COF of these composites were decreased due to the small number of deteriorated layers from the worn surface.

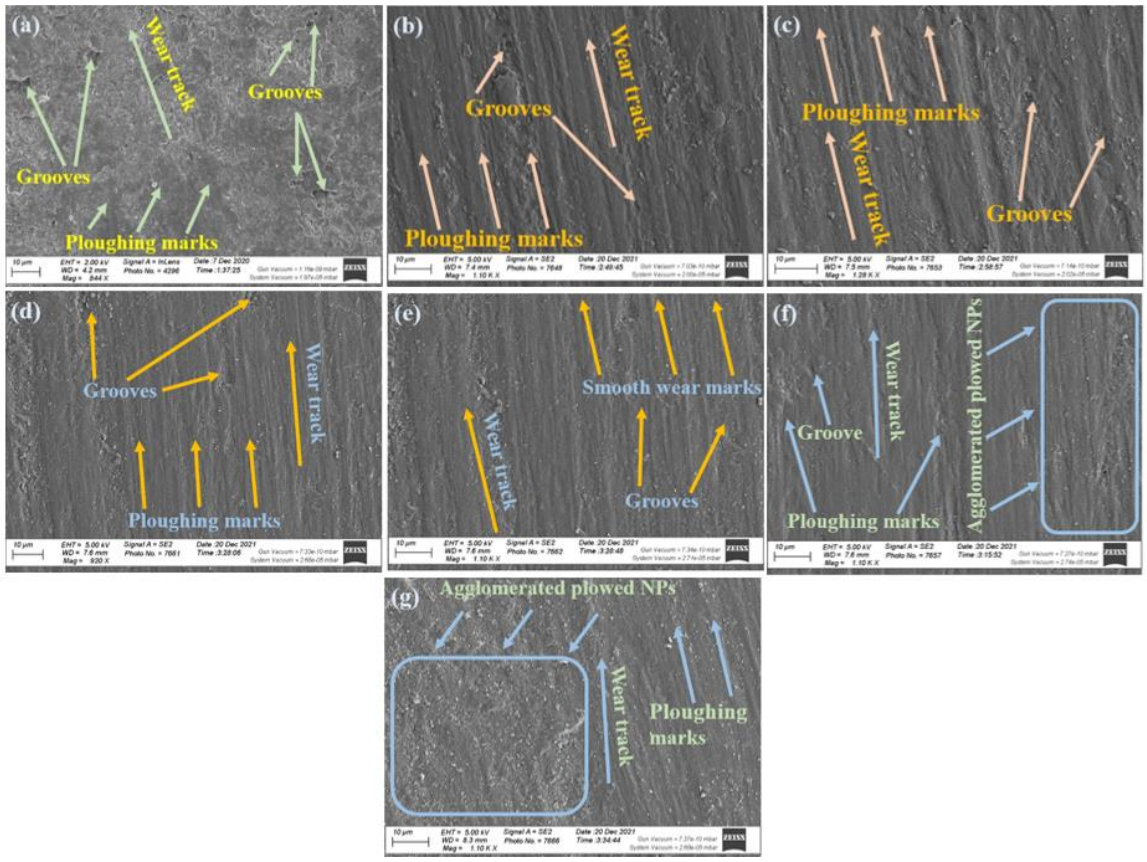

Fig. 10 SEM of worn surfaces after the wear test: a) unfilled PMMA, b) non-hybrid composites of C1, c) non-hybrid composites of C2, d) hybrid-nanocomposites of C1/0.4 wt. % DS NPs, e) hybrid-nanocomposites of C2/0.4 wt. % TiO_2 NPs, f) hybrid-nanocomposites of C1/0.5 wt. % DS NPs, and g) hybrid-nanocomposites of C2/0.5 wt. % TiO_2 NPs.

Also, Figs 10 d and e indicates the worn surfaces of hybrid nanocomposites of C1/0.4 wt. % DS NPs and C2/0.4 wt. % TiO_2 NPs, respectively. As observed from Figs 10 d and e, the worn surfaces smoothness of hybrid nanocomposites increased with

increasing hybrid NPs content up to 0.4 wt. %. Consequently, the surface morphology of hybrid nanocomposites changed from having deep wear marks to small wear marks. This can be attributed to the load carying capacity of the hybrid NPs as well as the large hardness and strength of PMMA hybrid-composites that led to an enhancement in the wear resistance and COF. Also, the high surface mechanical properties of hybrid composites at loading of 0.4 wt. % NPs have a prominent role in preventing the formation of deep wear marks on the worn surface. Besides surface characteristics, the transfer films that formed during sliding process also play an important role in enhancing the wear behaviour of the materials, [62]. The mixture of hybrid NPs (TiO_2/DS NPs) were easily released from the PMMA/hybrid NPs nanocomposites and transferred between the counterface, and the hybrid nanocomposites contact zone. Thus, these hybrid NPs act as modifiers and self-lubricating material between the contacting surfaces during the sliding process, and then prevented the direct contact between them, [63]. Therefore, the less wear marks and small grooves on the worn surfaces of the hybrid nanocomposites were observed, which led to increasing wear resistance and a clear reduction in the COF results. Hence, the hybrid nanocomposites exhibited the highest mechanical and tribological properties at hybrid NPs content of 0.4 wt. % compared to non-hybrid composites of C1 and C2. After increasing of hybrid NPs content up to 0.5 wt. %, the wear marks and grooves on the worn surfaces of hybrid C1/ 0.5 wt. % DS NPs and C2/0.5 wt. % TiO_2 NPs composites began to increase again, as shown in Figs 10 f and g, respictevely. As mentioned previously, when the hybrid NPs content exceeds 0.4 wt. %, they tend to agglomerate and aggregate in some areas of the specimen surface. Therefore, the worn surfaces shows greater roughness and wear marks compared to the hybrid NPs content of 0.4 wt. %. As a result, the COF increased as well as the wear resistance and surface hardness decreased.

Economic Analysis for PMMA-Based Hybrid NPs Costs.

Considering the nanocomposites manufacturing costs, we found that decreasing nanofillers costs decreases that of manufacturing. Based on the aforementioned results, the hybrid nanocomposites achieved remarkable improvement percentages in the mechanical and tribological properties compared to the non-hybrid composites, as shown in Fig. 11. Hence, the hybrid composites containing 1.2 wt. % DS NPs (C2/0.4 wt. % TiO_2 NPs) showed a higher mechanical and tribological improvement than the hybrid composites containing 1.2 wt. % TiO_2 NPs. It is worth noting that date seeds are cheap materials, and the cost of 1 kg of nano-sized DS is approximately $15. While the price of 1 kg of TiO_2 NPs is approximately $65. Therefore, the unit cost of hybrid samples containing of 1.2 wt. % TiO_2 NPs and 0.4% DS NPs is $0.00168 per unit. Also, the unit cost of hybrid samples containing 1.2 wt. % DS NPs and 0.4 wt. % TiO_2 NPs is $0.00088 per unit. Although the unit cost of the hybrid C2/0.4 wt. % TiO_2 NPs composites decreased by 47.6 % compared to the unit cost of the hybrid C1/0.4 wt. % DS NPs composites, it achieved a significant improvement in the mechanical and tribological properties, as shown in Fig. 11.Therefore, the hybrid composites containing 1.2 wt. % of organic fillers are considered an ideal choice for denture base applications economically, mechanically, and tribologically.

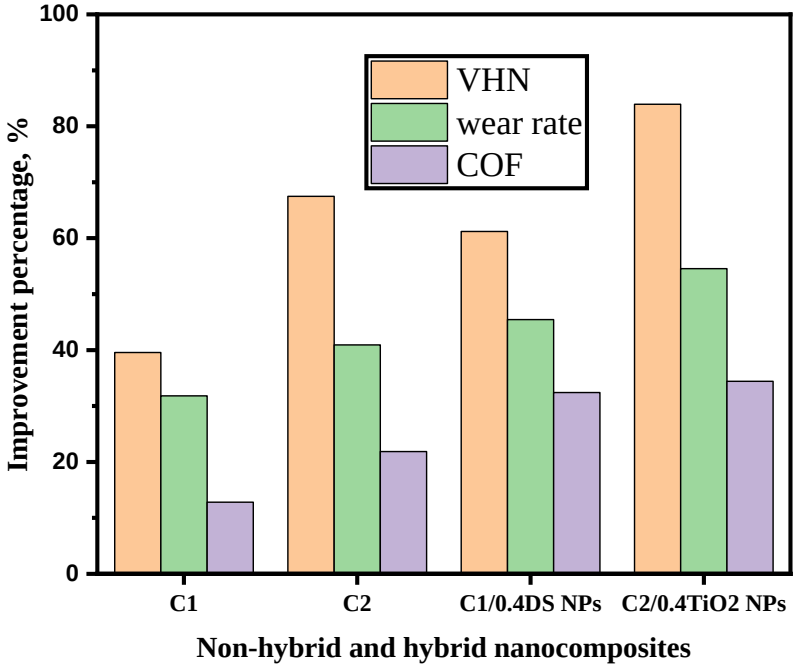

Fig. 11 Improvement percentages in the VHN, wear rate, and COF for hybrid and non-hybrid nanocomposites compared to unfilled PMMA.

CONCLUSIONS

In the present study, two types of hybrid NPs, DS and TiO_2 were used as reinforcement material of PMMA/1.2 wt. % TiO_2 NPs (C1) and PMMA/1.2 wt. % DS NPs (C2) composites, respectively. It was concluded that the non-hybrid composites of C1 and C2 showed higher mechanical and tribological properties than that of unfilled PMMA. VHN, wear rate, and COF of C1 were improved by 39.56, 31.81, and 12.81 % compared with the unfilled PMMA, respectively. Also, for C2, VHN, wear rate, and COF were improved by 67.47, 40.9, and 21.87 % compared with pure PMMA, respectively. Experimental results indicated that the mechanical and tribological properties of C1 and C2 were enhanced by adding hybrid NPs content up to 0.4 wt. %. Therefore, after addition of 0.4 wt. % DS NPs to C1 composites, the VHN, wear rate, and COF were improved by 15.49, 20.0, and 22.47 %, respectively compared with C1 composites. Also, the hybrid nanocomposites of C2/0.4 wt. % TiO_2 NPs exhibit improvement percentages of VHN, wear rate, and COF by 9.84, 23.07, and 16.05 %, respectively compared to non-hybrid composites of C2. Moreover, the hybrid nanocomposites of C2/0.4 wt. % TiO_2 NPs showed significant improvement by 14.12, 16.66, and 2.96 % in the VHN, wear rate, and COF, respectively compared to the hybrid nanocomposites of C1/0.4 wt. % DS NPs. Also, the unit cost of the hybrid nanocomposites of C2/0.4 wt. % TiO_2 NPs is lower than that of the hybrid nanocomposites of C1/0.4 wt. % DS NPs by 47.61%.

ACKNOWLEDGEMENTS

This work was supported by composite materials lab, production technology department, faculty of technology and education, Beni-Suef University, Egypt.

REFERENCES

1. M. M. Gad, S. M. Fouda, F. A. Al-Harbi, R. Näpänkangas, and A. Raustia, "PMMA denture base material enhancement: A review of fiber, filler, and nanofiller addition," Int. J. Nanomedicine, vol. 12, pp. 3801–3812, (2017).

2. M. M. Gad et al., "Effects of Denture Cleansers on the Flexural Strength of PMMA Denture Base Resin Modified with ZrO2 Nanoparticles," J. Prosthodont., vol. 30, no. 3, pp. 235–244, (2021)

3. N. G. Chander and J. Venkatraman, "Mechanical properties and surface roughness of chitosan reinforced heat polymerized denture base resin," J. Prosthodont. Res., vol. 66, no. 1, pp. 101–108, (2022).

4. M. I. Fayad, G. M. Alwafi, R. A. Abdelrahim, and A. A. Shon, "COLOUR STABILITY , FLEXURAL MODULUS , AND TOUGHNESS OF PMMA DENTURE BASE RESIN MODIFIED WITH SILVER NANO-PAR- TICLES AND HENNA FILLERS," vol. 25, no. 1, pp. 15–22, (2022).

5. M. Alqahtani and S. B. Haralur, "Influence of different repair acrylic resin and thermocycling on the flexural strength of denture base resin," Med., vol. 56, no. 2, pp. 1–9, (2020).

6. M. Chhabra, M. Nanditha Kumar, K. N. RaghavendraSwamy, and H. M. Thippeswamy, "Flexural strength and impact strength of heat-cured acrylic and 3D printed denture base resins- A comparative in vitro study," J. Oral Biol. Craniofacial Res., vol. 12, no. 1, pp. 1–3, Jan., (2022).

7. A. Takaichi et al., "A systematic review of digital removable partial dentures. Part II: CAD/CAM framework, artificial teeth, and denture base," J. Prosthodont. Res., vol. 66, no. 1, pp. 53–67, (2022).

8. S. Zidan, N. Silikas, J. Haider, A. Alhotan, J. Jahantigh, and J. Yates, "Evaluation of equivalent flexural strength for complete removable dentures made of zirconia-impregnated PMMA nanocomposites," Materials (Basel)., vol. 13, no. 11, (2020).

9. M. M. Gad et al., "Influence of artificial aging and ZrO2 nanoparticle-reinforced repair resin on the denture repair strength," J. Clin. Exp. Dent., vol. 12, no. 4, pp. e354–e362, (2020).

10. N. Prajwala, C. Ravi Kumar, M. Sujesh, D. Chalapathi Rao, and L. Pavani, "Denture base reinforcing materials - A review," IP Ann. Prosthodont. Restor. Dent., vol. 6, no. 2, pp. 52–59, Jun., (2020).

11. R. Giti, M. Firouzmandi, N. Zare Khafri, and E. Ansarifard, "Influence of different concentrations of titanium dioxide and copper oxide nanoparticles on water sorption and solubility of heat-cured PMMA denture base resin," Clin. Exp. Dent. Res., no. September 2021, pp. 1–7, (2022).

12. R. Adhikari and G. H. Michler, "Polymer nanocomposites characterization by microscopy," Polym. Rev., vol. 49, no. 3, pp. 141–180, (2009).

13. L. M. A. Meng T. R., "Physical properties of four acrylic denture base resins," J Contemp Dent Pr. 2005;693–100., vol. 6, no. 4, pp. 1–5, (2005).

14. A. E. S. M. HASSAN, M. N. EL-SHEIKH, W. Y. ALI, and M. N. M. ROHIM, "Mechanical and tribological performance of self-cured poly methyl methacrylate reinforced by alumina nanowires and zirconia nanoparticles for denture applications," Mater. Plast., vol. 58, no. 3, pp. 109–120, (2021).

15. R. Roy, "PURPOSIVE DESIGN OF NANOCOMPOSITES: ENTIRE CLASS OF NEW MATERIALS," Mater. Sci. Res., vol. 21, pp. 25–32, (1987).
16. M. Z. Rong, M. Q. Zhang, Y. X. Zheng, H. M. Zeng, R. Walter, and K. Friedrich, "Structure-property relationships of irradiation grafted nano-inorganic particle filled polypropylene composites," Polymer (Guildf)., vol. 42, no. 1, pp. 167–183, (2001).
17. J. Jordan, K. I. Jacob, R. Tannenbaum, M. A. Sharaf, and I. Jasiuk, "Experimental trends in polymer nanocomposites - A review," Mater. Sci. Eng. A, vol. 393, no. 1–2, pp. 1–11, (2005).
18. F. Shakeri, A. Nodehi, and M. Atai, "PMMA/double-modified organoclay nanocomposites as fillers for denture base materials with improved mechanical properties," J. Mech. Behav. Biomed. Mater., vol. 90, pp. 11–19, Feb., (2019).
19. P. Chaijareenont, H. Takahashi, N. Nishiyama, and M. Arksornnukit, "Effect of different amounts of 3-methacryloxypropyltrimethoxysilane on the flexural properties and wear resistance of alumina reinforced PMMA," Dent. Mater. J., vol. 31, no. 4, pp. 623–628, (2012).
20. Al-Saleh et al., "Use of Photosensitizer, Glutaraldehyde, alcohol and Ultrasonics in disinfection of polished and rough surfaces of self-curing polymethyl methacrylate denture base material," Photodiagnosis Photodyn. Ther., vol. 37, no. September, (2021).
21. A. A. M. N. Garcia et al., "Nanoparticle-modified PMMA to prevent denture stomatitis: a systematic review," Arch. Microbiol., vol. 204, no. 1, Jan., (2022)
22. G. Ergun, Z. Sahin, and A. S. Ataol, "The effects of adding various ratios of zirconium oxide nanoparticles to poly(methyl methacrylate) on physical and mechanical properties," J. Oral Sci., vol. 60, no. 2, pp. 304–315, (2018).
23. J. Kosmaca et al., "Investigating the mechanical properties of GeSn nanowires," Nanoscale, vol. 11, no. 28, pp. 13612–13619, (2019).
24. D. Mohammed and M. Mudhaffar, "Effect of modified zirconium nano-fillers addition on some properties of heat cured acrylic denture base material," J Bagh Coll. Dent., vol. 24, no. 4, pp. 1–7, (2012).
25. B. S. Jasim and I. J. Ismail, "The Effect of Silanized Alumina Nano - Fillers Addition on Some Physical and Mechanical Properties of Heat Cured Polymethyl Methacrylate Denture Base Material," J. Baghdad Coll. Dent., vol. 26, no. 2, pp. 18–23, (2014).
26. S. A. Alwan and S. S. Alameer, "The Effect of the Addition of Silanized Nano Titania Fillers on Some Physical and Mechanical Properties of Heat Cured Acrylic Denture Base Materials," J. Baghdad Coll. Dent., vol. 27, no. 1, pp. 86–91, (2015).
27. L. Ghahremani, S. Shirkavand, F. Akbari, and N. Sabzikari, "Tensile strength and impact strength of color modified acrylic resin reinforced with titanium dioxide nanoparticles," J. Clin. Exp. Dent., vol. 9, no. 5, pp. e661–e665, May, (2017).
28. A. Sodagar, A. Bahador, S. Khalil, A. Saffar Shahroudi, and M. Zaman Kassaee, "The effect of TiO2 and SiO2 nanoparticles on flexural strength of poly (methyl methacrylate) acrylic resins," J. Prosthodont. Res., vol. 57, no. 1, pp. 15–19, (2013).
29. I. M. Hamouda and M. M. Beyari, "Addition of glass fibers and titanium dioxide nanoparticles to the acrylic resin denture base material: comparative study with the conventional and high impact types.," Oral Health Dent. Manag., vol. 13, no. 1, pp.

107–12, (2014).
30. S. Rashahmadi, R. Hasanzadeh, and S. Mosalman, "Improving the Mechanical Properties of Poly Methyl Methacrylate Nanocomposites for Dentistry Applications Reinforced with Different Nanoparticles," Polym. - Plast. Technol. Eng., vol. 56, no. 16, pp. 1730–1740, (2017).
31. A. Alrahlah, H. Fouad, M. Hashem, A. A. Niazy, and A. AlBadah, "Titanium Oxide (TiO2)/polymethylmethacrylate (PMMA) denture base nanocomposites: Mechanical, viscoelastic and antibacterial behavior," Materials (Basel)., vol. 11, no. 7, (2018).
32. S. Issa Salih, J. Kadhim Oleiwi, and A. Saad Mohamed, "INVESTIGATION OF MECHANICAL PROPERTIES OF PMMA COMPOSITE REINFORCED WITH DIFFERENT TYPES OF NATURAL POWDERS," vol. 13, no. 22, (2018).
33. S. E. Salih, J. K. Oleiwi, and A. MohammedT, "Investigation of Hardness and Flexural Properties of PMMA Nano Composites and PMMA Hybrids Nano Composites Reinforced by Different Nano Particles Materials used in Dental Applications," (2016).
34. G. Petrone and V. Meruane, "Mechanical properties updating of a non-uniform natural fibre composite panel by means of a parallel genetic algorithm," Compos. Part A Appl. Sci. Manuf., vol. 94, pp. 226–233, Mar., (2017).
35. S. M. Mirabedini and K. Khodabakhshi, "Nanocomposites of PU Polymers Filled With Spherical Fillers," in Polyurethane Polymers: Composites and Nanocomposites, Elsevier Inc., (2017).
36. H. I. Elkhouly, R. K. Abdel-Magied, and M. F. Aly, "Date palm seed as suitable filler material in glass–epoxy composites," Iran. Polym. J. (English Ed., vol. 28, no. 1, pp. 65–73, Jan., (2019).
37. H. I. Elkhouly, R. K. Abdel-Magied, and M. F. Aly, "An investigation of date palm seed as effective filler material of glass–epoxy composites using optimization techniques," Polym. Polym. Compos., vol. 28, no. 8–9, pp. 541–553, Oct., (2020).
38. H. I. Elkhouly, "Comparison of the effects of nano date seed as reinforcement material for medium-density polyethylene (MDPE) and polyethylene terephthalate (PET) using multilevel factorial design," Polym. Polym. Compos., vol. 29, no. 9, pp. 1462–1471, (2021).
39. H. I. Elkhouly, E. M. Ali, M. N. El-Sheikh, and A. E.-S. M. Hassan, "An investigated organic and inorganic reinforcement as an effective economical filler of poly (methyl methacrylate) nanocomposites," Sci. Rep., vol. 12, no. 1, pp. 1–13, (2022).
40. A. O. Alhareb, H. M. Akil, and Z. A. Ahmad, "Mechanical Properties of PMMA Denture Base Reinforced by Nitrile Rubber Particles with Al2O3/YSZ Fillers," Procedia Manuf., vol. 2, no. February, pp. 301–306, (2015).
41. Y. Yao and Y. Zhou, "Effects of deep cryogenic treatment on wear resistance and structure of GB 35CrMoV steel," Metals (Basel)., vol. 8, no. 7, pp. 1–11, (2018).
42. A. E.-S. M. Hassan, A. I. EiD, M. El-Sheikh, and W. Y. Ali, "Effect of Graphene Nanoplatelets and Paraffin Oil Addition on the Mechanical and Tribological Properties of Low-Density Polyethylene Nanocomposites," Arab. J. Sci. Eng., vol. 43, no. 3, pp. 1435–1443, (2018).
43. A. E. M. Hassan, A. I. EiD, M. El-Sheikh, and W. Y. Ali, "Mechanical and tribological performance of polyamide 12 reinforced with graphene nanoplatelets and

paraffin oil nanocomposites," Materwiss. Werksttech., vol. 50, no. 1, pp. 74–85, (2019).
44. H. I. Elkhouly, M. A Rushdi, and R. K Abdel-Magied, "Eco-friendly date-seed nanofillers for polyethylene terephthalate composite reinforcement," Mater. Res. Express, vol. 7, no. 2, (2020).
45. N. N. Hafizah, M. H. Mamat, M. H. Abidin, C. M. S. Said, and M. Rusop, "Bonding and mechanical properties of PMMA/TiO2 nanocomposites," Adv. Mater. Res., vol. 832, pp. 700–705, (2014).
46. E. E. Totu, A. C. Nechifor, G. Nechifor, H. Y. Aboul-Enein, and C. M. Cristache, Poly(methyl methacrylate) with TiO2 nanoparticles inclusion for stereolitographic complete denture manufacturing − the fututre in dental care for elderly edentulous patients?, vol. 59. Elsevier Ltd, (2017).
47. S. Wang, M. Wang, Y. Lei, and L. Zhang, "`Anchor effect' in poly(styrene maleic anhydride)/TiO2 nanocomposites," J. Mater. Sci. Lett., vol. 18, no. 24, pp., (2009).
48. Y. Chen, H. Xu, and T. Sun, "Preparation and study of PMMA/TiO2 nanocomposites," Adv. Mater. Res., vol. 233–235, pp. 1830–1833, (2011).
49. I. A. Rahman, P. Vejayakumaran, C. S. Sipaut, J. Ismail, and C. K. Chee, "Size-dependent physicochemical and optical properties of silica nanoparticles," Mater. Chem. Phys., vol. 114, no. 1, pp. 328–332, (2009).
50. W. M. Aframehr, B. Molki, R. Bagheri, P. Heidarian, and S. M. Davodi, Characterization and enhancement of the gas separation properties of mixed matrix membranes: Polyimide with nickel oxide nanoparticles, vol. 153. Institution of Chemical Engineers, (2020).
51. I. L. Ali, N. Yunus, and M. I. Abu-Hassan, "Hardness, flexural strength, and flexural modulus comparisons of three differently cured denture base systems," J. Prosthodont., vol. 17, no. 7, pp. 545–549, (2008).
52. M. Alamgir, A. Mallick, G. C. Nayak, and S. K. Tiwari, "Development of PMMA/TiO2 nanocomposites as excellent dental materials," J. Mech. Sci. Technol., vol. 33, no. 10, pp. 4755–4760, (2019).
53. S. S. Fometu, Q. Ma, J. J. Wang, J. Guo, L. Ma, and G. Wu, "Biological Effect Evaluation of Different Sized Titanium Dioxide Nanoparticles Using Bombyx mori (Silkworm) as a Model Animal," Biol. Trace Elem. Res., no. 0123456789, (2022).
54. M. Cascione et al., "Improvement of pmma dental matrix performance by addition of titanium dioxide nanoparticles and clay nanotubes," Nanomaterials, vol. 11, no. 8, (2021).
55. J. Orellana, I. Moreno-villoslada, R. K. Bose, F. Picchioni, M. E. Flores, and R. Araya-hermosilla, "Self-healing polymer nanocomposite materials by joule effect," Polymers (Basel)., vol. 13, no. 4, pp. 1–24, (2021).
56. A. Nabhan, M. Taha, and N. M. Ghazaly, "Filler loading effect of Al2O3/TiO2 nanoparticles on physical and mechanical characteristics of dental base composite (PMMA)," Polym. Test., vol. 117, no. October 2022, p. 107848, (2023).
57. Z. bing Cai, M. hao Zhu, S. Yang, X. biao Xiao, X. zhou Lin, and H. yang Yu, "In situ observations of the real-time wear of PMMA flat against steel ball under torsional fretting," Wear, vol. 271, no. 9–10, pp. 2242–2251, (2011).
58. M. N. Rohim, M. N. El-Sheikh, W. Y. Ali, and A. E.-S. M. Hassan, "Effect of Al2O3 Nanowires and ZrO2 Nanoparticles Addition on the Mechanical and

Tribological Properties of Heat-Cured PMMA Acrylic Denture Base Material," High Temp., vol. 24, p. 28, (2021).
59. E. Hornbogen, "Role of Fracture Toughness in the Wear of Metals.," Wear, vol. 33, no. 2, pp. 251–259, (1975).
60. A. L. M. Costa, A. C. C. Reis, L. Kestens, and M. S. Andrade, "Ultra grain refinement and hardening of IF-steel during accumulative roll-bonding," vol. 406, pp. 279–285, (2005).
61. A. M. Sadoun, A. Fathy, A. Abu-oqail, H. T. Elmetwaly, and A. Wagih, "Structural , mechanical and tribological properties of Cu – ZrO2 / GNPs hybrid nanocomposites," Ceram. Int., no. November, pp. 0–1, (2019).
62. B. P. Chang, H. M. Akil, M. G. Affendy, A. Khan, and R. B. M. Nasir, "Comparative study of wear performance of particulate and fiber-reinforced nano-ZnO/ultra-high molecular weight polyethylene hybrid composites using response surface methodology," Mater. Des., vol. 63, pp. 805–819, (2014).
63. L. Chang, Z. Zhang, H. Zhang, and K. Friedrich, "Effect of nanoparticles on the tribological behaviour of short carbon fibre reinforced poly (etherimide) composites," vol. 38, pp. 966–973, (2005).